Journal of Instrumentation

The study of *in vivo* x-ray fluorescence (XRF) technique for gadolinium (Gd) measurements in human bone

To cite this article: F. Mostafaei and L.H. Nie 2016 *JINST* **11** T08001

Jinst

Published by IOP Publishing for Sissa Medialab

Received: *June 16, 2016*
Accepted: *July 26, 2016*
Published: *August 2, 2016*

TECHNICAL REPORT

The study of *in vivo* x-ray fluorescence (XRF) technique for gadolinium (Gd) measurements in human bone

F. Mostafaei[a,b,1] **and L.H. Nie**[a]

[a] *School of Health Sciences, Purdue University, West Lafayette, IN 47907, U.S.A.*
[b] *Departement of Radiation Oncology, Medical College of Wisconsin, Milwaukee, WI 53226, U.S.A.*

E-mail: fmostafa@purdue.edu

Abstract: An *in vivo* K x-ray fluorescence system, based on ^{109}Cd source, for the detection of gadolinium has been investigated. Gd is of interest because of the extensive use of Gd-based contrast agents in MR imaging. A human simulating bone phantom set has been developed. The phantoms were doped with seven concentrations of Gd. Additional elements important for *in vivo* x-ray fluorescence, Na, Cl and Ca, were also included to create an overall elemental composition consistent with the Reference Man. A new 5 GBq ^{109}Cd source was purchased to improve the source activity in comparison to the previous study (0.17 GBq). The previously published minimum detection limit (MDL) for Gd phantom measurements using KXRF system was 3.3 ppm. In this study the minimum detection limit for bare bone phantoms was found to reduce the MDL to 0.8, a factor of 4.1. The previous published data used only three layers of plastic as soft tissue equivalent materials and found the MDL of 4–4.8 ppm. In this study we have used the plastic with more realistic thicknesses to simulate a soft tissue at tibia. The detection limits for phantoms with Lucite as a tissue equivalent, using a new source, was determined to be 1.81 to 3.47 ppm (μg Gd per gram phantom). Our next study would be testing an *in vivo* K x-ray fluorescence system, based on ^{109}Cd source on human volunteers who went through MR imaging and were injected by Gd.

Keywords: X-ray fluorescence (XRF) systems; X-ray generators and sources

[1] Corresponding author.

doi:10.1088/1748-0221/11/08/T08001

2016 JINST 11 T08001

Contents

2016 JINST 11 T08001

1 Introduction

Gadolinium-based contrast agents has used clinically as a contrast enhancement agent in magnetic resonance imaging (MRI). Gadolinium is a rare earth element of the lanthanide group ($Z = 64$) which is used to shorten T_1 relaxation times in the tissue [3, 7, 13]. Darrah et al. study showed the ability of releasing and integrating of free Gd^{3+} ions into the body [4]. Gd longevity within the body is more complicated than previously believed. A study done by Noseworthy et al. 2002 demonstrates the fact that Gd enters vascular endothelial cells after an acute Gd-chelate injection [18]. Study done by Kanda 2013 confirms the connection between Gd and abnormalities in two regions of brain, which represents the Gd toxicity in the brain [11]. Another study by Japanese researcher Kanda 2015, confirmed the existence of Gd contrast in the brains for people who have received contrast-enhanced MRI [10]. Previous studies demonstrated the possibility of long-term retention and toxicity of Gd in bone [1, 21]. The biological half-life for Gd in bone mineral has been estimated to be 3500 days [9]. Darrah et al. study showed the Gd chelates are cleared from the body after 90 minutes of injection [4], and almost 1–2% of injected gadodiamide (Gd-DTPA-BMA) was reported to be stored in bone for longer than 8 years [2, 4]. Studies showed the use of Gd as a contrast agent can increase the risk of Nephrogenic Systemic Fibrosis (NSF) in patients with renal disease [6, 12, 22]. Gd concentrations of 0.7 to 10 ppm have been measured *in-vitro* on the femoral head of patients who had undergone hip replacement surgery. These patients were injected by Gd previously as a contrast enhanced MRI scans [4, 23].

In order to find the amount of Gd in bone *in-vivo*, a noninvasive method using bone phantom and x-ray-fluorescence (XRF) system to assess Gd retention was investigated.The amount of Gd could be of importance in studies of Gd retention and thus assessment of exposure and potential toxicity.

2 Method

The ^{109}Cd source with activity of 5 GBq, which is mounted coaxially in a tungsten cup on the front of a four-detector 'clover-leaf' array, was used. This source emits 88 keV γ-rays and a series of silver x-rays at 22 keV. The detectors only measure the signal that is scattered back from the phantoms (180° or backscatter geometry). A 0.5 mm copper is placed in front of the tungsten cup to reduce the silver x-ray signal by 99.99%, while only reducing the 88 keV γ-rays by 25%. The four detectors are coaxial p-type hyperpure germanium (HPGe) low-energy photon detectors (model GL0210S, CANBERRA) which are 16 mm in diameter and 10 mm thick. The signals from the HPGe detectors are processed with four digital pulse processing systems (DSA-1000) and logged into separate spectra in a computer. The geometry of the four detectors is shown in figure 1.

Figure 1. A photograph the four HPGe detectors. A Gd phantom is shown placed in front of the system.

A set of seven phantoms were made using $GdCl_3.6H_2O$ (Sigma-Aldrich, St. Louis, MO) as the doping agent with concentrations of 0, 5, 10, 20, 40, 80 and 100 ppm Gd. The compounds $NaNO_3$ (1.29 g of Na), NH_4Cl (1.2 g of Cl), $CaSO_4.1/2H_2O$ (13.9 g of Ca) were also included in the phantoms in order to maintain a trace element composition consistent with Reference Man [4]. Mowiol® 4-88 [20] was used as a binder [15, 16]. The phantoms are mixed to create a homogenous distribution of gadolinium and calcium. The units of concentration used are the mass of gadolinium per unit mass of phantom. The phantoms are made as cylinder shape with 3 cm radius and 3 cm height.

The phantom set was first measured bare i.e. with no overlying soft-tissue material over the bone to simulate bare bone measurements. The phantom set was then measured with soft-tissue-equivalent nine plastic sheets (Lucite), with thicknesses of 0.61, 1.09, 1.7, 2.18, 2.79, 3.28, 3.89, 5.01 and 6.13 mm, placed between the phantom and the ^{109}Cd source to simulate an *in vivo* measurement where soft tissue overlies the bone. Phantoms (both bare and with plastic overlay) were all measured for 3600 s real time.

2016 JINST 11 T08001

The effective and the equivalent dose to a subject's leg for one hour measurement was 0.26 μSv, and 0.714 mSv respectively [17]. This dose is negligible in comparison to maximum annual effective dose limit (5 mSv) and doses associated with standard medical imaging procedures (e.g. the dose for a typical chest x-ray is about 0.1 mSv).

For each measurement four spectra were obtained from the detection system, which consists of four detectors. The Gd x-ray peak contains two areas ($K\alpha_1$ = 42.9962 keV and $K\alpha_2$ = 42.3089 keV). The peak fitting algorithm was used to extract the Gd x-ray peak areas. Therefore, for each phantom concentration eight x-ray peak areas were obtained. Calibration lines were constructed using the Gd counts versus Gd concentration (ppm) to calculate the minimum detection limit.

The Levenberg-Marquardt fitting algorithm was used to extract peak areas and the analysis was programmed by Matlab. We initially fitted the data with an equation of 8 parameters (six for the Gaussian peaks and two for the exponential background). In this study, the fitting was found to be improved (determined by an improved chi-square) with a reduced number of parameters. Therefore, our results were obtained by fitting with a reduced number of parameters. The same width, fixed relative position (in terms of energy) and fixed ratio area were chosen for both Gaussian peaks. Therefore, both x-ray peaks were fitted by five parameters (three Gaussian parameters and two parameters for the exponential background):

$$y = B\exp(mx) + \frac{A_1}{\sigma_1\sqrt{2\pi}}\exp\left(-\frac{1}{2}\left(\frac{x-x_a}{\sigma_1}\right)^2\right) + \frac{0.56A_1}{\sigma_1\sqrt{2\pi}}\exp\left(-\frac{1}{2}\left(\frac{x-(x_a+13.66)}{\sigma_1}\right)^2\right)$$

Where, y represents the count rate (s^{-1}) and m represents the slope of the exponential background, B is the intercept of exponential background, A_1 is the peak area, σ_1 is the peak widths (standard deviation), x_a is the peak centroids, $13.66 = \frac{\text{Energy difference between two peaks}}{\text{Gain}}$ and 0.56 is the intensity ratio of $K\alpha_2/K\alpha_1$. To maintain stability of all the fits for the spectra obtained from the detectors, the peak widths and centroid positions were constrained to fall within 0.5 standard deviations of the values determined from the highest concentration peaks.

The minimum detectable limit (MDL) was calculated in the following manner.

$$\text{MDL} = \frac{2\times\sqrt{\text{background}}}{\text{slope}}$$

Four estimates of the Gd concentrations which were extracted from four spectra were obtained from each phantom. Therefore, the total counts estimated for gadolinium phantoms were calculated from equation (2.1). The total uncertainty (σ) was calculated by equation (2.2) as a weighted average of all of the estimates. The weighted average taking the slight differences in the detectors performance (the uncertainties on some estimates are better than others) into account.

A total count estimated and uncertainty for gadolinium phantoms was calculated in the following manner:

$$\text{Total counts estimated for each phantom} = \frac{\left(\frac{\chi_1}{(\sigma_1)^2}\right)+\left(\frac{\chi_2}{(\sigma_2)^2}\right)+\left(\frac{\chi_3}{(\sigma_3)^2}\right)+\left(\frac{\chi_4}{(\sigma_4)^2}\right)}{\left(\frac{1}{(\sigma_1)^2}\right)+\left(\frac{1}{(\sigma_2)^2}\right)+\left(\frac{1}{(\sigma_3)^2}\right)+\left(\frac{1}{(\sigma_4)^2}\right)} \tag{2.1}$$

$$\sigma = \sqrt{\frac{1}{\left(\frac{1}{(\sigma_1)^2}\right)+\left(\frac{1}{(\sigma_2)^2}\right)+\left(\frac{1}{(\sigma_3)^2}\right)+\left(\frac{1}{(\sigma_4)^2}\right)}} \tag{2.2}$$

2016 JINST 11 T08001

Where χ_1 to χ_4 are the numbers of counts and σ_1 to σ_4 are the uncertainties, which were obtained from each phantom by different detectors. Figure 2 shows the Gd spectral shape.

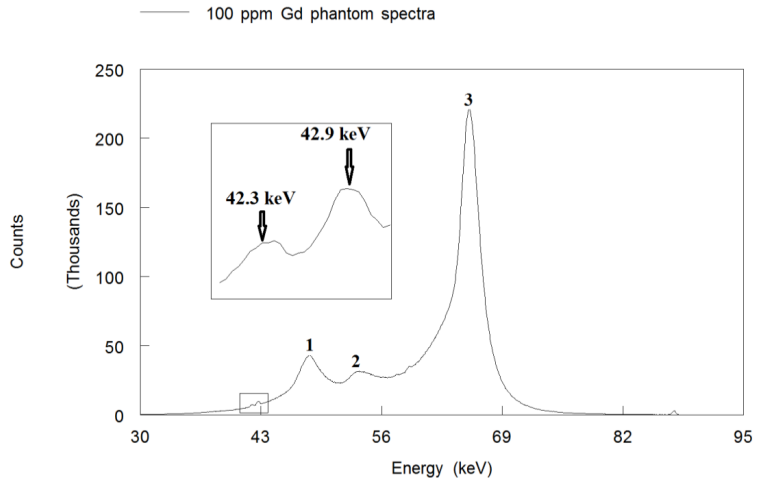

Figure 2. XRF spectra from 100 ppm Gd phantom (1: Compton back-scattered tungsten x-rays from the source collimator, 2: Compton back-scattered photons passing through the detector and then backscattered back into the detector (Compton of the Compton = $\frac{E_\gamma}{1+\frac{E_\gamma}{0.511}(1-\cos 180)}$, $E_\gamma = 66$ keV), 3: Compton peak).

3 Results

3.1 Using bare bone phantoms

A set of seven phantoms with different amount of Gd concentration were measured. The calibration line of the x-ray signal for the bare bone phantoms are shown in figure 3 (error bars are too small and cannot be seen on the graph). The minimum detection limit from x-ray signals was determined via the inverse weighting method as previously described and found to be 0.8 ppm.

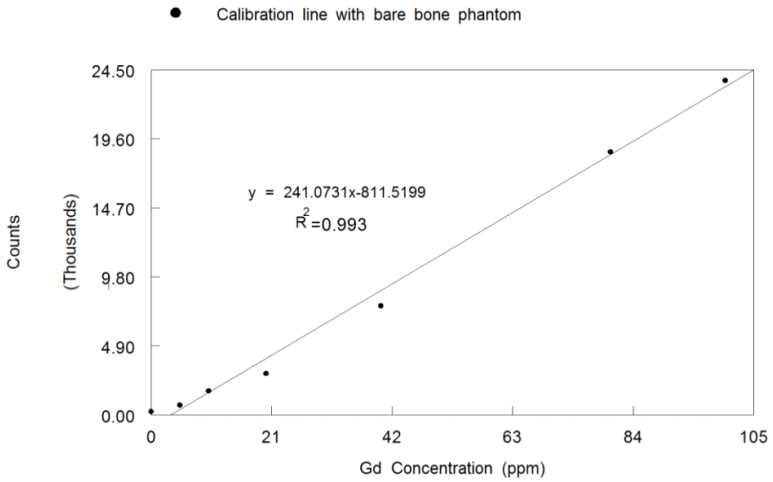

Figure 3. Phantom Calibration line for bare bone phantom.

2016 JINST 11 T08001

3.2 Soft tissue phantoms

Bare bone phantom with an overlay of soft tissue equivalent plastic sheets (Lucite with 0.61, 1.09, 1.7, 2.18, 2.79, 3.28, 3.89, 5.01 and 6.13 mm) were examined. Pejović-Milić et al, 2002 study showed the average tissue thickness of 4.8 mm at tibia [19]. Layers of plastic were used and placed between the bare bone phantom and ^{109}Cd source, they were measured for one hour (figure 4). Table 1 shows the Gd MDLs for these phantoms. The minimum detection limit of bone phantoms with soft tissue was found to be a factor of 2.2–4.3 poorer than using the bare bone phantom. These differences are regarding to the γ-rays and x-rays attenuation due to overlying tissue, and also the phantom's distance from the source and phantom's distance from the detectors which increase by adding each plastic sheet. The distances from source to phantom, and phantom to the detector were 5 mm and 10 mm respectively. The calibration lines of the Gd x-ray signal for bone phantoms with adding each layer of Lucite are shown in figure 5.

Figure 4. The 6.13 mm Lucite is shown placed between Gd phantom and detection system.

Table 1. Gadolinium phantom minimum detection limit determined from x-ray peaks for different tissue overlay thicknesses.

Lucite Thickness (mm)	**0.61**	**1.09**	**1.7**	**2.18**	**2.79**	**3.28**	**3.89**	**5.01**	**6.13**
Inverse Variance Weighted MDL (ppm)	1.81	2.16	2.33	2.56	2.73	2.85	3.03	3.22	3.47

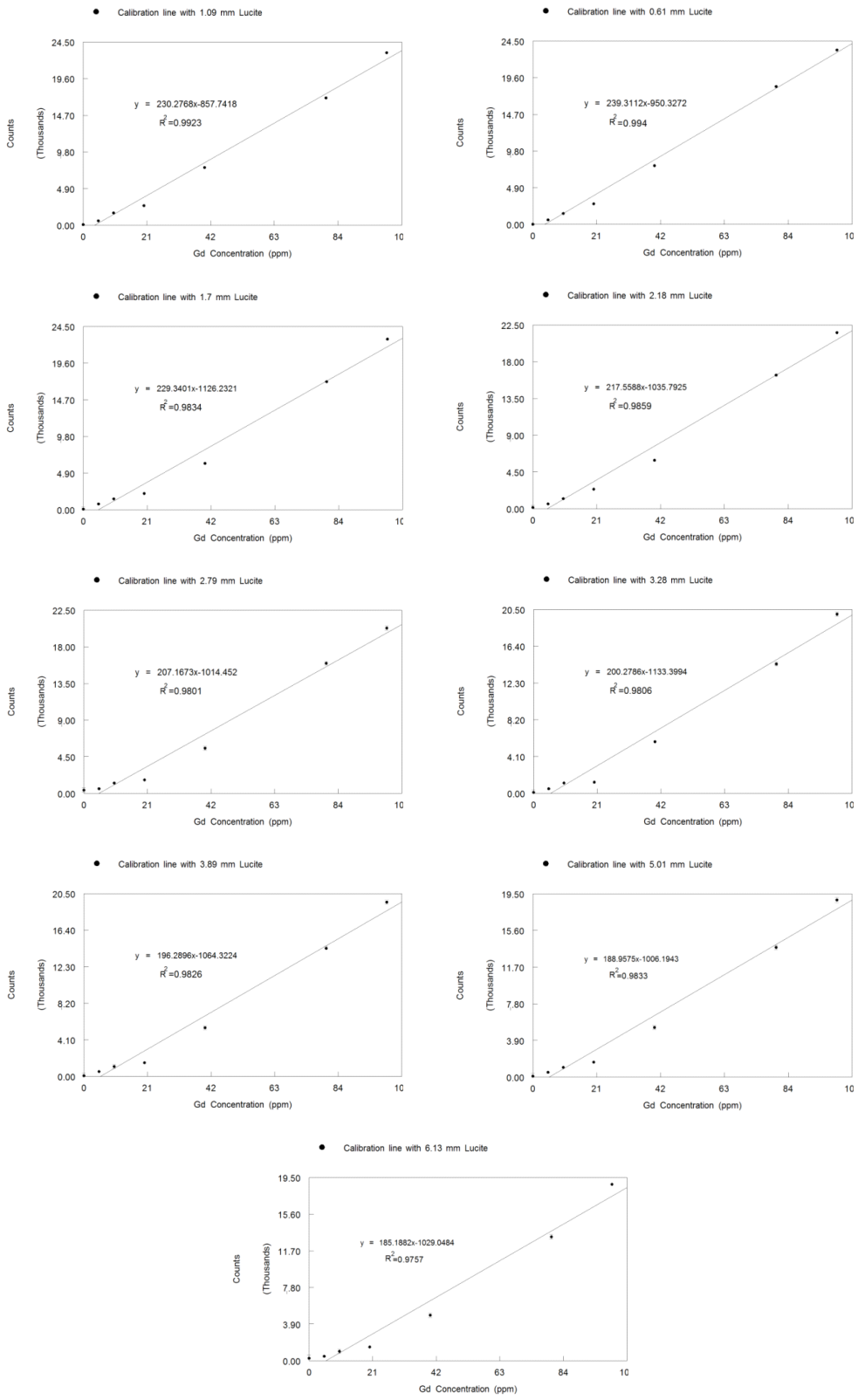

Figure 5. Calibration lines with adding Lucite to simulate soft tissue.

4 Discussions

The results were constructed from 5 parameters (same width, fixed relative position and fixed ratio area) in Gaussian peaks. Physically, $K\alpha_1$ and $K\alpha_2$ intensities are correlated, the intensities' ratio is about 0.56 ($K\alpha_2/K\alpha_1$) therefore these peaks were analyzed together [24]. Also, reduction in uncertainty was achieved as the number of parameters was reduced.

Bone phantom measurements show that dead time is in the range 11–16% with a 5 GBq source. To estimate the number of counts and MDL, and also have a comparison with previous study, the increased counts with a 5 GBq source instead of 0.17 GBq in the same real time measurement period (3600 s) can be estimated slightly conservatively to be $0.84 \times 5/0.17 = 24.7$. The MDL can be predicted to be lowered by the square root of this figure, or a factor of 4.9. Mostafaei et al. 2015 study the MDL was found to be 3.3 ppm for bare bone phantom using 0.17 GBq ^{109}Cd source [14]. In this study MDL was found to be 0.8 ppm, which is improved by factor of 4.1. The small deviation was observed between predicted MDL (calculated theoretically) from previous study and measured MDL in this study. This should be due to differences in dead time used in calculation and correction. Also, by using 0.17 GBq source, the MDL with 2–4 mm of overlying skin thicknesses was predicted to be 6.1 to 8.6 ppm in previous study [14]. With a new 5GBq ^{109}Cd source the MDL with more realistic overlying skin thicknesses of 0.61–6.13 mm of Lucite as tissue equivalent was found to be 1.8 to 3.47 ppm.

The levels of Gd in the bone of patients who received Gd contrast agent were reported as low as 0.7–10 ppm which was measured by *in-vitro* method [5, 23]. The MDL lies within the range of measured levels of found in patients administered Gd imaging agents. Hence, the system can be used on volunteers who went through MR imaging procedure and used Gd as a contrast agent.

5 Conclusions

A series of improvements have been undertaken to a system for the measurement of gadolinium in bone *in vivo*.

1. an improvement in minimum detection limit resulting from using stronger source (5 GBq instead of 0.17 GBq) of a factor of 4.1;
2. the development of better fitting algorithm (using 5 parameters instead of 8 parameters in Gaussian peaks) which improved the uncertainty and MDL;
3. the use of more plastics as soft tissue equivalent to simulate an actual soft tissue at tibia and to have more realistic measurements;

The ^{109}Cd γ-ray based K-XRF system now has an in phantom detection limit of 0.8 ppm compared to a previous detection limit of 3.3 ppm. The system can now be tested on human volunteers to see if individuals who received Gd contrast agent can be distinguished using this technique.

Acknowledgments

This work was supported by the National Institute for Occupational Safety and Health (NIOSH) R21 grants 1R21OH010044 and 1R21OH010700 and the Purdue University Nuclear Regulatory Commission (NRC) Faculty Development Grant NRC-HQ-11-G-38-0006.

The authors declare that there is no conflict of interests regarding the publication of this paper.

2016 JINST 11 T08001

References

[1] J.L. Abraham, C. Thakral, L. Skov, K. Rossen and P. Marckmann, *Dermal inorganic gadolinium concentrations: evidence for in vivo transmetallation and long-term persistence in nephrogenic systemic fibrosis*, *Brit. J. Dermatol.* **158** (2008) 273.

[2] S. Aime and P. Caravan, *Biodistribution of gadolinium-based contrast agents, including gadolinium deposition*, *J. Magn. Reson. Im.* **30** (2009) 1259.

[3] L. Calabi, G. Alfieri, L. Biondi, M. De Miranda, L. Paleari and S. Ghelli, *Application of High-Resolution Magic-Angle Spinning NMR Spectroscopy to Define the Cell Uptake of MRI Contrast Agents*, *J. Magn. Reson.* **156** (2002) 222.

[4] T.H. Darrah, J.J. Prutsman-Pfeiffer, R. J. Poreda, M. Ellen Campbell, P.V. Hauschka and R.E. Hannigan, *Incorporation of excess gadolinium into human bone from medical contrast agents*, *Metallomics* (2009) **1** 479.

[5] W.A. Gibby, K.A. Gibby and W.A. Gibby, *Comparison of Gd DTPA-BMA (Omniscan) versus Gd HP-DO3A (ProHance) Retention in Human Bone Tissue by Inductively Coupled Plasma Atomic Emission Spectroscopy*, *Invest. Radiol.* **39** (2004) 138.

[6] T. Grobner, *Gadolinium-a specific trigger for the development of nephrogenic fibrosing dermopathy and nephrogenic systemic fibrosis*, *Nephrol. Dial. Transplant.* **21** (2006) 1104.

[7] R.E. Hendrick and E.M. Haacke, *Basic physics of MR contrast agents and maximization of image contrast*, *J. Magn. Reson. Im.* **3** (1993) 137.

[8] *Report of the Task Group on Reference Man: A Report*, ICRP Publication 23, Pergamon Press, Oxford (1975).

[9] *Limits for intakes of radionuclides by workers*, *Ann. ICRP* **6** (1981) 67.

[10] T. Kanda, H. Oba, K. Toyoda, K. Kitajima and S. Furui, *Brain gadolinium deposition after administration of gadolinium-based contrast agents*, *Jpn. J. Radiol.* **34** (2015) 3.

[11] T. Kanda, K. Ishii and H. Kawaguchi, *High signal intensity in the dentate nucleus and globus pallidus on unenhanced T1-weighted MR images: relationship with increasing cumulative dose of a gadolinium-based contrast material*, *Radiology* **270** (2014) 834.

[12] P. Marckmann et al., *Nephrogenic systemic fibrosis: suspected causative role of gadodiamide used for contrast-enhanced magnetic resonance imaging*, *J. Am. Soc. Nephrol.* **17** (2006) 2359.

[13] F. Mostafaei, F.E. McNeill, D.R. Chettle, M.D. Noseworthy and W.V. Prestwich, *The feasibility of in vivo quantification of bone-gadolinium in humans by prompt gamma neutron activation analysis (PGNAA) following gadolinium-based contrast-enhanced MRI*, *Radiat. Phys. Chem. 116* (2015) 248.

[14] F. Mostafaei, F.E. McNeill, D.R. Chettle, M.D. Noseworthy, *A feasibility study to determine the potential of in vivo detection of gadolinium by x-ray fluorescence (XRF) following gadolinium-based contrast-enhanced MRI*, *Physiol. Meas.* **36** (2015) N1-N13.

[15] F. Mostafaei, F.E. McNeill, D.R. Chettle and W.V. Prestwich, *Improvements in an in vivo neutron activation analysis (NAA) metod for the measurement of fluorine in human bone*, *Physiol. Meas.* **34** (2013) 1329.

[16] F. Mostafaei, F.E. McNeill, D. R. Chettle, W.V Prestwich and M. Inskip, *Design of a phantom equivalent to measure bone-fluorine in a human's hand via delayed neutron activation analysis*, *Physiol. Meas.* **34** (2013) 503.

2016 JINST 11 T08001

[17] H. Nie, D. Chettle, L. Luo and J. O'Meara, *Dosimetry study for a new in vivo X-ray fluorescence (XRF) bone lead measurement system*, *Nucl. Instrum. Meth.* **B 263** (2007) 225.

[18] M.D. Noseworthy, C. Ackerley, X. Qi and G.A. Wright, *Correlating subcellular contrast agent location from dynamic contrast-enhanced magnetic resonance imaging (dMRI) and analytical electron microscopy*, *Acad. Radiol. 9* (2002) S514.

[19] A. Pejović-Milić, J. A. Brito, J. Gyorffy and D.R. Chettle, *Ultrasound measurements of overlying soft tissue thickness at four skeletal sites suitable for in vivo x-ray fluorescence*, *Med. Phys.* **29** (2002) 2687.

[20] Polysciences Inc, *Mowiol® 4-88*, data sheet 777, (2008).

[21] C. Thakral, J. Alhariri and J.L. Abraham, *Long-term retention of gadolinium in tissues from nephrogenic systemic fibrosis patient after multiple gadolinium-enhanced MRI scans: case report and implications*, *Contrast Media Mol. I.* **205** (2007) 199.

[22] H. Thomsen, S. Morcos and P. Dawson, *Is there a causal relation between the administration of gadolinium based contrast media and the development of nephrogenic systemic fibrosis (NSF)*, *Clin. Radiol.* **61** (2006) 905.

[23] G.W. White, W.A. Gibby and M.F. Tweedle, *Comparison of Gd (DTPA-BMA) (Omniscan) Versus Retention in Human Bone Tissue by Inductively Coupled Plasma Mass Spectroscopy*, *Invest. Radiol.*, 41 (2006) 272.

[24] *X-ray Data Booklet* (2009), http://xdb.lbl.gov/Section1/Table_1-3.pdf.

2016 JINST 11 T08001